HHS Public Access

Author manuscript

Biol Psychiatry. Author manuscript; available in PMC 2022 May 01.

Published in final edited form as:

Biol Psychiatry. 2021 May 01; 89(9): 857–867. doi:10.1016/j.biopsych.2020.11.021.

Amygdala and Insula Connectivity Changes Following Psychotherapy for Posttraumatic Stress Disorder: A Randomized Clinical Trial

Gregory A. Fonzo, Ph.D.[1,*], **Madeleine S. Goodkind, Ph.D.**[2,*], **Desmond J. Oathes, Ph.D.**[3], **Yevgeniya V. Zaiko, B.A.**[4,5,6], **Meredith Harvey, B.A.**[4,5,6], **Kathy K. Peng, B.S.**[4,5,6], **M. Elizabeth Weiss, Ph.D.**[4,5,6], **Allison L. Thompson, Ph.D.**[4], **Sanno E. Zack, Ph.D.**[4], **Steven E. Lindley, M.D. Ph.D.**[4,6], **Bruce A. Arnow, Ph.D.**[4], **Booil Jo, Ph.D.**[4], **Barbara O. Rothbaum, Ph.D.**[7], **Amit Etkin, M.D., Ph.D.**[4,5,8]

[1]Department of Psychiatry, The University of Texas at Austin Dell Medical School

[2]New Mexico Veterans Affairs Healthcare System, Albuquerque, NM, USA

[3]Center for Neuromodulation in Depression and Stress, Department of Psychiatry, University of Pennsylvania Perelman School of Medicine, Philadelphia, PA, USA

[4]Department of Psychiatry and Behavioral Sciences, Stanford University School of Medicine, Stanford, CA, USA

[5]Wu Tsai Neurosciences Institute, Stanford University, Stanford CA, USA

[6]Veterans Affairs Palo Alto Healthcare System, and the Sierra Pacific Mental Illness, Research, Education, and Clinical Center (MIRECC), Palo Alto, CA

[7]Trauma and Anxiety Recovery Program, Department of Psychiatry, Emory University School of Medicine, Atlanta, GA, USA

[8]Alto Neuroscience, Inc., Los Altos, CA USA

Correspondence To: Amit Etkin, M.D., Ph.D., 477 South San Antonio Road, Los Altos, CA 94022; amitetkin@altoneuroscience.com; 650-725-5736.

*Equal contributions as first authors

Author contributions: Dr. Fonzo had full access to all the data in the study and takes responsibility for the integrity of the data and the accuracy of the data analysis. Drs. Fonzo and Goodkind contributed equally to this research. The author contributions are as follows: concept and design (Dr. Etkin); acquisition, analysis, and interpretation of data (all authors); drafting of the manuscript (Dr. Fonzo); critical revision of the manuscript for important intellectual content (all authors); statistical analyses (Dr. Fonzo); obtained funding (Dr. Etkin); administrative, technical, or material support (Drs. Fonzo, Goodkind, Oathes, Lindley, Arnow, Jo, Rothbaum, and Etkin); supervision (Drs. Weiss, Thompson, Zack, Rothbaum, and Etkin).

Role of the funder/sponsor: The National Institutes of Health had no role in the design and conduct of the study; the collection, management, analysis, and interpretation of the data; preparation, review, or approval of the manuscript; nor decision to submit the manuscript for publication.

Previous presentation(s) of reported material: Portions of this work have been previously presented at the Annual Conference for the American College of Neuropsychopharmacology (ACNP), Palm Springs, CA, USA, Dec. 3-7, 2017 and Hollywood, FL, USA, Dec. 9-13, 2018; and the Annual Conference of the Society of Biological Psychiatry (SOBP), San Diego, CA, USA, May 18-20, 2017; and Chicago, IL, USA, May 16-18, 2019.

Abstract

Background: Exposure-based psychotherapy is a first-line treatment for posttraumatic stress disorder (PTSD), but its mechanisms are poorly understood. Functional brain connectivity is a promising metric for identifying treatment mechanisms and biosignatures of therapeutic response. To this end, we assessed amygdala and insula treatment-related connectivity changes and their relationship to PTSD symptom improvements.

Method: Individuals (N=66) with a primary PTSD diagnosis participated in a randomized clinical trial of prolonged exposure therapy (N=36) vs. treatment waiting list (N=30). Task-free functional magnetic resonance imaging (fMRI) was completed prior to randomization and 1 month following cessation of treatment/waiting list. Whole-brain blood oxygenation level-dependent (BOLD) responses were acquired. Intrinsic connectivity was assessed, by subregion, in the amygdala and insula, limbic structures key to the disorder pathophysiology. Dynamic causal modeling (DCM) assessed evidence for effective connectivity changes in select nodes informed by intrinsic connectivity findings.

Results: The amygdala and insula displayed widespread patterns of primarily subregion-uniform intrinsic connectivity change, including increased connectivity between amygdala and insula; increased connectivity of both regions with the ventral prefrontal cortex, frontopolar, and sensory cortices; and decreased connectivity of both regions with left fronto-parietal nodes of the executive control network. Larger decreases in amygdala-frontal connectivity and insula-parietal connectivity were associated with larger PTSD symptom reductions. DCM evidence suggested treatment decreased left frontal inhibition of the left amygdala, and larger decreases were associated with larger symptom reductions.

Conclusions: PTSD psychotherapy adaptively attenuates functional interactions between frontoparietal and limbic brain circuitry at rest, which may reflect a potential mechanism or bio-signature of recovery.

ClinicalTrials.gov Name: Brain Imaging of Psychotherapy for Posttraumatic Stress Disorder (PTSD)

ClinicalTrials.gov Identifier: NCT01507948

ClinicalTrials.gov url: https://clinicaltrials.gov/ct2/show/NCT01507948

Keywords

IMAGING; PSYCHOTHERAPY; PTSD; FMRI; CONNECTIVITY; RESTING

Introduction

Post-traumatic stress disorder (PTSD) is a prevalent (1, 2), persistent (3), and highly impairing (4, 5) condition typically treated with a trauma-focused psychotherapy (6) such as prolonged exposure (PE), which is an empirically supported, exposure-based treatment for PTSD (7). Though efficacious (6, 8), a substantial number of individuals fail to respond (9). We also lack validated metrics to predict how an individual will respond to treatment and knowledge of how such treatments promote recovery.

Recently, functional magnetic resonance imaging (fMRI) has been used to identify brain function that changes with treatment and that predicts favorable treatment response (10). Non-invasive brain measurements can provide bio-behaviorally informative metrics (11, 12) and are therefore top contenders for biomarker development. Our work (13, 14) and that of others (15-19) utilizing task-based imaging has provided key insights regarding potential mechanisms by which psychotherapy promotes disorder recovery and the neural phenotypes for which these treatments are effective. However, the imaging metric perhaps best suited to biomarker development is resting state connectivity, as it is easy to acquire and can distinguish individual brain activity (11).

PTSD displays altered resting state connectivity of the amygdala (20, 21) and insula (22, 23), which are tightly coupled both structurally (24) and functionally (25) due to their common role in emotion processing (26) and defensive threat responses (27). Network-level disturbances have also been reported, such as reduced default mode network connectivity (28-30), enhanced salience network connectivity (including the amygdala and mid/posterior insula) (21, 23, 28, 31), and altered connectivity between these networks (22, 28, 29, 32). Studies assessing PTSD treatment-related resting state connectivity changes have primarily assessed seeded connectivity in limbic (33-35), prefrontal, and posterior medial seeds (34). Others have utilized mixed diagnostic samples to examine treatment-related changes in amygdala connectivity (36) and how these relate to depressive symptom reductions (37). Accumulated evidence suggests PTSD psychotherapy increases prefrontal-limbic connectivity (33, 35, 36) and connectivity between default mode and executive control networks (34, 35).

However, the existing evidence is characterized by several weaknesses, including use of experimental or poorly disseminated treatments (34, 35), lack of a patient control arm (33, 36, 37), and examination of multiple psychotherapies targeting different diagnoses (36, 37). Additionally, shared treatment-related connectivity changes of both the amygdala and insula have also not yet been identified. Both structures display tight structural (24) and functional interconnections (25), a common role in emotion processing (26) and threat detection (27), and common disorder-related abnormalities (38, 39). This suggests the possibility of a common pattern of treatment-related effects.

Here, we aimed to characterize intrinsic brain connectivity changes following PE for PTSD. We focused on connectivity of the amygdala and insula, as these limbic brain structures are heavily implicated in the pathophysiology of PTSD (40), display abnormal activation/connectivity (30, 38, 39, 41, 42), and have demonstrated treatment-predictive effects and treatment-related changes in PTSD imaging studies (13, 33, 36). To advance prior work, we employ a randomized clinical trial design with a patient waiting list (WL) control condition and maintained the intent-to-treat framework in our longitudinal mixed model analyses.

This report builds upon prior studies published on this same sample, including an investigation of emotional reactivity and emotion-regulation task-based fMRI moderators of PE vs. WL response (13) and pre/post changes (14), as well as identification of a treatment-resistant biological PTSD subtype defined by ventral attention network resting state connectivity and verbal memory (43). Task-based studies identified that, at baseline, greater

prefrontal and lower amygdala emotional reactivity-related brain responses as well as greater ventromedial prefrontal implicit emotion regulation-related brain responses predicted a more favorable response to PE vs. WL. In contrast, only left lateral frontopolar cortex activation during explicit emotion regulation, i.e. cognitive reappraisal showed a PE-specific increase that was associated with therapeutic response. Of note here, the prior resting state connectivity investigation of this sample did not at all examine amygdala and insula whole brain resting state connectivity changes (43).

Thus, our goals here were as follows. First, we sought to identify treatment-specific changes in subregional and region-uniform connectivity patterns of the amygdala and insula. Second, we aimed to identify connectivity changes common to both limbic structures, consistent with their shared functional roles (26, 27) and PTSD-related abnormalities (38, 39). Third, we aimed to identify how connectivity changes related to symptom reductions, thereby identifying potential limbic signatures of symptom remission. We also leveraged effective connectivity, a model of directed influence of one region on another, to explore evidence for treatment-related changes. For this purpose we utilized dynamic causal modeling (DCM) (44) for resting state fMRI (45), also known as spectral DCM. This is a powerful Bayesian modeling method for exploring directionality of influence in defined nodes. We reserved this method for exploratory *post hoc* modeling of effects in select loci informed by results from intrinsic connectivity analyses and did not undertake a comprehensive investigation.

We predicted that individuals randomized to PE vs. WL would display, at post-treatment, increased amygdala resting state connectivity with the ventromedial prefrontal cortex (vmPFC) (33); with the anterior insula/frontal operculum (33); and with the lateral prefrontal cortex (36). Beyond our focused hypotheses, we predicted that: a) additional treatment-related connectivity changes would be identified common to both the amygdala and insula, reflecting their shared roles in emotion processing (26) and functional (25) and structural connectivity (24); and b) additional analyses would identify shared connectivity changes associated with magnitudes of symptom improvement.

Methods

The following is an abbreviated description. Please see the Supplement for complete details.

Participants and Assessments

The study protocol was reviewed and approved by the Stanford University Institutional Review Board (IRB), and all study procedures were conducted in accordance with IRB and protocol guidelines. Trauma survivors, ages 18-60, eligible to undergo MRI, with good English comprehension, and meeting DSM-IV diagnostic criteria for PTSD were recruited to participate in a psychotherapy treatment study. Individuals with comorbid major depression and anxiety disorders were allowed to participate as long as PTSD was judged by study clinicians to be the primary clinical disorder. After receiving an explanation of study procedures and being given the opportunity to ask questions, participants provided written informed consent. All study procedures were reviewed and approved by the Stanford University Institutional Review Board. Trained PhD-level clinicians established DSM-IV

diagnoses using the Clinician-Administered PTSD Scale for PTSD (CAPS) (46) and the Structured Clinical Interview for DSM-IV Diagnosis (SCID-IV) (47).

Scan Acquisition

Eligible participants underwent fMRI on a separate day prior to randomization. Participants completed an 8 minute eyes-open resting state scan (240 volumes acquired) in which they were told to lie still, stay awake, focus on a fixation cross, and allow their mind to wander.

Randomization and Treatment

Participants were individually randomized via random number generator to either immediate PE treatment (n=36) or treatment WL (n=30). Participants randomized to immediate PE completed 9 to 12 sessions of prolonged exposure therapy (PE), which is an empirically supported exposure-based PTSD treatment (48). Participants in WL had a 10-week waiting period with minimal contact with study staff.

Post-Treatment Assessments

Approximately 4 weeks following the final PE session (or 10 weeks following the beginning of treatment WL), participants completed a post-treatment/post-waiting list clinical assessment and scan.

Image Processing Pipeline

Resting state BOLD sequences were pre-processed and analyzed using the CONN toolbox version 15.h (49) with the SPM 12 software package in Matlab R2019b. The default pre-processing pipeline was utilized, and images were smoothed with a 6.0 mm FWHM Gaussian kernel. Quality control settings for artifact rejection tools (ART toolbox) corresponded to the “Intermediate” setting (97^{th} percentile), which flagged volumes with global signal changes > 5 SD above the mean and framewise displacement > 0.9mm. Additional quality control cutoffs instituted were: a) no more than 4mm root mean square absolute displacement across the mean of the squared maximum displacements in each of the 6 estimated translational and rotational motion parameters across the entire run; and b) no more than 5% (12 volumes) of the entire run flagged to be censored from analysis.

Connectivity Seed Regions

Seed regions of interest (Figure S1) were defined utilizing established anatomical or functionally-parcellated brain maps of the amygdala (basolateral, centromedial, and superficial) (50) and insula (ventral anterior, dorsal anterior, and posterior) (51).

Seeded Connectivity Group Analysis

Connectivity maps for each structure’s subregions were subjected to a voxel wise linear mixed model (52). Effects of interest were differences in connectivity change between PE and WL that were uniform across subregions (time x treatment arm) and arm-differential changes in connectivity from pre- to post-treatment specific to a subregion (time x treatment arm x subregion). The F statistical maps for each effect were corrected for multiple comparisons utilizing a whole brain voxel level false discovery rate (FDR) correction ($q <$

0.025; Bonferroni-corrected for the two sets of seeded connectivity analyses). Baseline major depressive disorder (MDD) diagnosis was explored *post hoc* as a potential moderator of effects.

Relationship of Amygdala and Insula Connectivity Changes to Symptom Changes

To examine relationships between common amygdala and insula connectivity changes and symptom changes, we tested in a linear mixed model framework whether the effect of treatment on CAPS total score changes was moderated by amygdala and insula connectivity changes with targets displaying significant and congruent treatment-related increases or decreases, i.e. common effects identified via conjunction of amygdala and insula subregion-general Type I error-corrected effects maps. For each overlapping effect, a linear mixed model with a random intercept tested whether within-subject connectivity change (post vs. pre-treatment) moderated the effect of treatment (PE vs. WL) on time-related changes in CAPS (i.e. a treatment arm x time x connectivity change interaction effect). The effect of interest was this three-way interaction, which specifies differences in magnitude of treatment-related symptom change as a function of connectivity change. Bonferroni-correction across all clusters from the conjunction analysis was utilized to control for Type I error inflation due to multiple comparisons, yielding a posterior cutoff of $p < 0.0016$ (two-sided p of 0.05 divided by 16, 8 tests each for the amygdala and insula).

DCM Analyses

DCM was conducted according to previously published methods (53). Peaks of maximal low-frequency resting BOLD fluctuations were identified in the left and right amygdala and insula (Table S5), yielding four limbic foci of interest. Additional foci included the left inferior frontal junction (IFJ) and the left intraparietal sulcus (IPS), which were identified with linear mixed models to display treatment-related decreases in connectivity that were associated with treatment-related changes in symptoms. Inverted fully-connected models were then taken to second-level analyses with parametric empirical Bayes (PEB) (54) to assess evidence for network connections at pre-treatment and treatment arm x time effects. PEBs were then subjected to Bayesian model reduction (BMR) (55) and Bayesian model averaging (BMA) (56) to assess the posterior free energies for the presence vs. absence of each effect on each model parameter at the group level (57). An additional PEB with BMR and BMA was also implemented to identify effective connectivity changes that scaled with changes in PTSD symptoms.

Results

See Supplement for a more detailed description of results.

Sample Characteristics

The randomized sample encompassed 66 individuals with PTSD, with 36 randomized to PE and 30 randomized to WL (Figure S2). Arms were well matched on all clinical and demographic variables (Table 1). At baseline, 18 in the PE group and 17 in WL met diagnostic criteria for MDD. Of those randomized, 24 individuals in the immediate treatment arm and 26 individuals in waiting list underwent post-treatment assessments and

resting state scans. As expected, individuals randomized to PE displayed significantly larger reductions in PTSD symptoms from pre- to post-treatment relative to WL (Table 1).

Motion Estimates and Imaging Quality Control

Head motion during the resting state fMRI scan was within the quality control cutoffs at all time points and did not differ between groups. No participants were excluded from analyses for poor data quality or motion artifacts.

Treatment Effects on Intrinsic Connectivity

Amygdala—Subregion-uniform connectivity changes were widespread (Table S1; Figure S3), but there were no subregion-specific changes. As hypothesized, we observed significant treatment-related increases in amygdala connectivity bilaterally with the ventral anterior insula (Figure 1A), with the posterior vmPFC/orbitofrontal cortex (Figure 1B), and with the right anterior DLPFC/frontopolar cortex. However, more posterior regions of the DLPFC (bilateral middle frontal gyri and left inferior frontal junction; IFJ) showed treatment-related decreases. Additional observed effects included increased amygdala connectivity with the visual and sensory/motor cortices, and decreased connectivity with the cerebellum, posterior cingulate, angular gyri, and inferior parietal cortex. MDD diagnosis did not moderate treatment effects.

Insula—Subregion-uniform changes in insular connectivity patterns were widespread (Table S2; Figure S4), and there were also significant subregion-specific effects (Table S3). Convergent with amygdala findings, insular connectivity with the bilateral amygdalae was increased in the PE arm at post-treatment. Increased insular connectivity was also observed with a left posterior vmPFC/orbitofrontal region that appeared to overlap with an area demonstrating increased amygdala connectivity (Figure 1B). Additional effects included increased insula connectivity with visual and sensory-motor cortices, anterior DLPFC/frontopolar cortex, and inferior temporal cortices. Decreased connectivity was observed with the dorsal anterior cingulate, dorsomedial prefrontal cortex, the left more posterior DLPFC (middle frontal gyrus and left IFJ), the left inferior parietal cortex, and cerebellum. MDD diagnosis did not moderate treatment effects.

Common Amygdala and Insula Connectivity Changes—A conjunction analysis of Type I error-corrected effects maps revealed overlapping amygdala and insula connectivity changes (Table S4), including shared connectivity increases with the right dorsal frontopolar cortex, right and left primary sensory cortices, visual cortex, and left posterior vmPFC/orbitofrontal cortex. Shared connectivity decreases were observed with the left IFJ, left intraparietal sulcus (IPS), and cerebellum (Figure 2A).

Relationship of Intrinsic Connectivity Changes to Symptom Changes

After correction for multiple comparisons, we observed two significant effects (Figure 2B). First, greater decreases in connectivity between the amygdala and the left IFJ were associated with larger reductions in symptoms from pre- to post-treatment for PE vs. WL ($F = 10.99$, p = 0.0014; Figure 2B). This effect was specific to PE ($t = 2.86$, $p = 0.005$) and not WL ($t = -1.25$, $p = 0.22$). Second, greater decreases in connectivity between the insula and

the left IPS were associated with larger reductions in symptoms from pre- to post-treatment for PE vs. WL ($F = 11.25$, $p = 0.0013$; Figure 2B). This effect was likewise specific to PE ($t = 3.50$, $p = 0.001$) and not WL ($t = -1.19$, $p = 0.24$).

Treatment Effects on Effective Connectivity

DCM examined effective connectivity between left and right amygdala and insula foci of maximal low-frequency BOLD fluctuations (Table S5) as well as left IFJ and IPS, identified as showing common connectivity decreases that were related to symptom changes. At baseline, the DCM network was characterized by excitatory connections between limbic structures, and frontoparietal inhibitory connections to and from limbic structures (Supplement, Table S6, and Figure 3A). Treatment arm x time effects with posterior probabilities (Pp) > 0.99 (i.e. very strong evidence) were observed for 4 connections (Table S7), each described as follows for PE vs. WL at post- vs. pre-treatment (Figure 3B). First, the left amygdala displayed a larger decrease in inhibitory effect on the left insula. Second, the right amygdala displayed a larger decrease in inhibitory effect on the left IPS. Third, the left IFJ displayed a larger decrease in inhibitory effect on the left amygdala. Fourth, the left IPS displayed a greater increase in inhibitory effect on the left amygdala.

Relationship of Effective Connectivity Changes to Symptom Changes

Of connections displaying evidence of treatment-related effects, we observed very strong evidence ($Pp > 0.99$) for a positive relationship between CAPS total score reductions and reductions in the inhibitory effect of the left IFJ on the left amygdala, i.e. greater reductions in CAPS total scores were associated with larger pre- to post-treatment decreases in left IFJ inhibition of the left amygdala. Additionally, very strong evidence for relationships between CAPS reductions and treatment-related changes were observed for other connections (Table S8), but in both cases, greater reductions in CAPS were associated with connectivity changes in the opposite direction of treatment effects.

Discussion

Here, we examined how exposure therapy impacts intrinsic functional connectivity of two key limbic brain structures demonstrated to manifest disorder abnormalities (20, 23, 38, 39). We replicate findings for psychotherapy-related changes in amygdala connectivity, i.e. increased insula and vmPFC connectivity, and we strengthen these findings in the context of a randomized clinical trial of PE vs. WL. We extend prior work by demonstrating convergent treatment-related insula connectivity changes, including common decreased connectivity with left frontoparietal executive control network nodes (58), the IFJ and IPS. Finally, we show that treatment-related connectivity decreases between the amygdala and left IFJ and between the insula and left IPS scaled with symptom improvement. In aggregate, these findings provide strong evidence that trauma-focused psychotherapy promotes widespread shifts in the intrinsic functional architecture of limbic circuitry. Of these shifts, we identify reductions in limbic connectivity with frontoparietal regions in the resting brain state as a candidate therapeutic process to be enhanced or promoted with mechanistically-focused intervention approaches.

These findings offer unique insights beyond those provided by other published studies of this clinical trial (13, 14, 43), which have not at all investigated potential PE therapeutic mechanisms as indexed by amygdala and insula whole brain resting state connectivity. Of relevance here, we previously reported that more effective inhibition of the amygdala by the right DLPFC (as inferred by concurrent transcranial magnetic stimulation pulses and fMRI, as well as opposite patterns of predictive activation during an emotional reactivity task) predicted a more favorable response to PE vs. WL (13), which may appear contradictory to the current pattern of effects. However, relationships between neurobiological treatment-moderating characteristics and treatment-related changes are largely unknown. In inferring across these studies, we put forth the following model to be tested and refined in future work. We speculate that DLPFC inhibition of the amygdala at baseline represents an endogenous top-down compensatory process in some individuals to modulate bottom-up limbic reactivity, which (in conjunction with greater degree of vmPFC-facilitated implicit regulation of emotion) facilitates optimal engagement with PE (13). As therapeutic relief is garnered with treatment engagement, we hypothesize this endogenous cortico-limbic reactivity-related compensatory process is less generalized to non-emotional contexts (e.g., the resting state), which manifests as an observed connectivity reduction (as seen here). This may be secondary to emergence of an intra-frontal emotion regulation enhancement characterized by increased lateral frontopolar cortex deployment and enhanced connectivity with vmPFC implicit regulatory circuitry during explicit emotion regulation, consistent with our prior findings for therapy-related brain changes during cognitive reappraisal (14), or perhaps it results from an enhancement of amygdala and insula resting state connectivity with the vmPFC (as seen here). The current findings thus provide critical additional evidence to contextualize our prior reports (13, 14) and thereby further our understanding of how cortical-limbic interactions serve to facilitate benefit and display context-dependent change following efficacious psychotherapy.

Consistent with prior work, we found psychotherapy increased amygdala and insula intrinsic connectivity following PE (33). A hyper-connectivity abnormality has been previously reported between these regions (21, 28, 31), though the location is generally reported to be in the mid/posterior insula, not the anterior region where we and others (33) observed treatment-related connectivity increases. We also replicate findings for increased connectivity of the amygdala with the vmPFC following PE (33), though the effect we detected was more posterior and sat at the intersection of the ventral striatum, olfactory cortex, and subgenual cingulate (Brodmann area 25). The insula also displayed connectivity increases with this same posterior vmPFC site. This novel finding suggests the posterior vmPFC bordering the striatum and subgenual cingulate functions more coherently at rest with these limbic structures following treatment. We speculate this change may accompany or occur in response to the decreased connectivity observed with IFJ and IPS nodes, potentially representing an adaptive shift in limbic regulation from a dorsal frontoparietal stream to a ventral prefrontal stream, a balance previously found to be disturbed in PTSD (59, 60).

We detected increased amygdala and insula connectivity with portions of the anterior DLPFC/frontopolar cortex, which partially converges with prior findings for increased connectivity with other portions of the inferior frontal gyrus (36). However, this frontopolar

region falls into the default mode network (58), which is not consistent with prior work (36) that observed changes in DLPFC portions of the executive control network. In contradistinction (36), we noted treatment-related decreases of limbic connectivity with a posterior DLPFC region on the left side, the IFJ, which aggregates with the executive control network at rest (58). This area, located at the interface of the inferior frontal sulcus and inferior precentral sulcus, is well known to play a key role in multiple forms of top-down cognitive control (61). We interpret this change to be indicative of the aforementioned shift in limbic-prefrontal dynamics from a treatment-facilitating, compensatory dorsal frontoparietal top-down interaction towards one largely mediated by ventral prefrontal structures that are typically highly connected at rest with limbic networks (62). A prior study (36) noted a qualitatively different effect in a separate portion of the DLPFC, but that study also differed in key ways (mixed diagnostic sample, two psychotherapy treatments targeting different primary diagnoses, no patient control group, and a different analytic strategy).

We likewise observed evidence for treatment-related changes in effective connectivity amongst limbic and frontoparietal nodes. These effective connectivity findings should be considered preliminary and hypothesis-generating, as we did not undertake a comprehensive modeling approach to assessing effective connectivity changes (63, 64). The choice of nodes in a network can impact the directionality and magnitude of connections, and which nodes to include is largely determined by the experiment, prior knowledge, and hypotheses (65). We modeled the bilateral amygdalae, bilateral insulae, IFJ, and IPS to explore treatment effects on effective connectivity informed by intrinsic connectivity treatment-related adaptive changes as well as prior knowledge for functional relationships and interconnections amongst these regions (66-71), and a larger network more inclusive of additional brain structures may have yielded different insights. However, we feel the primary contribution of this analysis is to generate hypotheses and motivate additional research into limbic-prefrontal directional interactions utilizing experimental brain probes (e.g., transcranial magnetic stimulation or focused ultrasound) concurrent with a brain readout in PTSD prior to and following evidence-based treatment, which will provide more definitive evidence in regards to directionality of change in limbic-prefrontal interactions. Worthy of note, here, was strong evidence for a reduced inhibitory effect of the left IFJ on the left amygdala, with additional strong evidence that greater reductions were associated with more favorable treatment responses. This converges with the intrinsic connectivity reductions observed between the left IFJ and amygdala that also scaled with treatment response, suggesting that intrinsic connectivity may index a change in the degree to which the left IFJ is exerting an inhibitory effect on the amygdala. This would be consistent with the hypothesized working model for a treatment-related shift in prefrontal-limbic connectivity.

Limitations are as follows: first, we did not have a trauma-exposed healthy comparison group that underwent repeated brain assessments, which would facilitate inference on psychotherapy-related normalization of PTSD brain abnormalities and development of compensatory adaptations. Second, we focused on treatment effects in a limited subset of the total possible connectivity features able to be examined. Thus, additional treatment-related changes may remain undetected in our more focused search, but we felt this would be the most judicious approach to yield potentially important insights into treatment mechanisms. Third, we investigated only one active treatment (PE), and as such these findings may not be

specific to PE or psychotherapy and may reflect therapeutic mechanisms shared with other treatment modalities. Future studies are needed to clarify the specificity or commonality of these effects with other PTSD treatments.

In conclusion, successful PTSD psychotherapy results in a widespread reorganization of limbic functional architecture, including an adaptive connectivity reduction with top-down frontoparietal control regions. These findings serve to clarify the nature of limbic-prefrontal interactions in PTSD that predict and change with treatment, and, when integrated with prior findings, suggest a new conceptual model for how psychotherapy reorganizes brain function. This work provides testable hypotheses which may yield novel mechanistic targets for future intervention optimization.

Supplementary Material

Refer to Web version on PubMed Central for supplementary material.

Acknowledgments

Funding and support: Supported by NIMH grant R01 MH091860 to Dr. Etkin. Dr. Fonzo was partially supported by NIMH grant T32 MH019938, by NIMH grant K23 MH114023, and by the Office of Academic Affiliations, Advanced Fellowship Program in Mental Illness Research and Treatment, Department of Veterans Affairs.

Financial Disclosures

Dr. Rothbaum has received funding from the Wounded Warrior Project, the Department of Defense (Clinical Trial Grant W81XWH-10-1-1045), and McCormick Foundation. Dr. Rothbaum receives royalties from Oxford University Press, Guilford, APPI, and Emory University and received advisory board payments from Genentech, Jazz Pharmaceuticals, Nobilis Therapeutics, Neuronetics, and Aptinyx. Dr. Fonzo owns equity in Alto Neuroscience. Dr. Etkin receives equity and salary from Alto Neuroscience, and has equity in Akili Interactive, Mindstrong Health and Sizung. The other authors report no biomedical financial interests or potential conflicts of interest.

References

1. Hoge CW, Riviere LA, Wilk JE, Herrell RK, Weathers FW (2014): The prevalence of post-traumatic stress disorder (PTSD) in US combat soldiers: a head-to-head comparison of DSM-5 versus DSM-IV-TR symptom criteria with the PTSD checklist. The lancet Psychiatry. 1:269–277. [PubMed: 26360860]
2. Kessler RC, Aguilar-Gaxiola S, Alonso J, Benjet C, Bromet EJ, Cardoso G, et al. (2017): Trauma and PTSD in the WHO World Mental Health Surveys. European journal of psychotraumatology. 8:1353383. [PubMed: 29075426]
3. Marmar CR, Schlenger W, Henn-Haase C, Qian M, Purchia E, Li M, et al. (2015): Course of Posttraumatic Stress Disorder 40 Years After the Vietnam War: Findings From the National Vietnam Veterans Longitudinal Study. JAMA Psychiatry. 72:875–881. [PubMed: 26201054]
4. Kessler RC, Sonnega A, Bromet E, Hughes M, Nelson CB (1995): Posttraumatic stress disorder in the National Comorbidity Survey. Archives of general psychiatry. 52:1048–1060. [PubMed: 7492257]
5. Schnurr PP, Lunney CA, Bovin MJ, Marx BP (2009): Posttraumatic stress disorder and quality of life: extension of findings to veterans of the wars in Iraq and Afghanistan. Clinical psychology review. 29:727–735. [PubMed: 19744758]
6. Cusack K, Jonas DE, Forneris CA, Wines C, Sonis J, Middleton JC, et al. (2016): Psychological treatments for adults with posttraumatic stress disorder: A systematic review and meta-analysis. Clinical psychology review. 43:128–141. [PubMed: 26574151]

7. Foa EB, Gillihan SJ, Bryant RA (2013): Challenges and Successes in Dissemination of Evidence-Based Treatments for Posttraumatic Stress: Lessons Learned From Prolonged Exposure Therapy for PTSD. Psychological science in the public interest: a journal of the American Psychological Society. 14:65–111. [PubMed: 25722657]
8. Bradley R, Greene J, Russ E, Dutra L, Westen D (2005): A multidimensional meta-analysis of psychotherapy for PTSD. Am J Psychiatry. 162:214–227. [PubMed: 15677582]
9. Schottenbauer MA, Glass CR, Arnkoff DB, Tendick V, Gray SH (2008): Nonresponse and dropout rates in outcome studies on PTSD: review and methodological considerations. Psychiatry. 71:134–168. [PubMed: 18573035]
10. Malejko K, Abler B, Plener PL, Straub J (2017): Neural Correlates of Psychotherapeutic Treatment of Post-traumatic Stress Disorder: A Systematic Literature Review. Frontiers in psychiatry. 8:85. [PubMed: 28579965]
11. Finn ES, Shen X, Scheinost D, Rosenberg MD, Huang J, Chun MM, et al. (2015): Functional connectome fingerprinting: identifying individuals using patterns of brain connectivity. Nat Neurosci. 18:1664–1671. [PubMed: 26457551]
12. Shah LM, Cramer JA, Ferguson MA, Birn RM, Anderson JS (2016): Reliability and reproducibility of individual differences in functional connectivity acquired during task and resting state. Brain and behavior. 6:e00456. [PubMed: 27069771]
13. Fonzo GA, Goodkind MS, Oathes DJ, Zaiko YV, Harvey M, Peng KK, et al. (2017): PTSD Psychotherapy Outcome Predicted by Brain Activation During Emotional Reactivity and Regulation. Am J Psychiatry. 174:1163–1174. [PubMed: 28715908]
14. Fonzo GA, Goodkind MS, Oathes DJ, Zaiko YV, Harvey M, Peng KK, et al. (2017): Selective Effects of Psychotherapy on Frontopolar Cortical Function in PTSD. Am J Psychiatry. 174:1175–1184. [PubMed: 28715907]
15. Felmingham K, Kemp A, Williams L, Das P, Hughes G, Peduto A, et al. (2007): Changes in anterior cingulate and amygdala after cognitive behavior therapy of posttraumatic stress disorder. Psychological science. 18:127–129. [PubMed: 17425531]
16. Lindauer RJ, Booij J, Habraken JB, Meijel EP, Uylings HB, Olff M, et al. (2008): Effects of psychotherapy on regional cerebral blood flow during trauma imagery in patients with post-traumatic stress disorder: a randomized clinical trial. Psychological medicine. 38:543–554. [PubMed: 17803835]
17. Thomaes K, Dorrepaal E, Draijer N, de Ruiter MB, Elzinga BM, van Balkom AJ, et al. (2012): Treatment effects on insular and anterior cingulate cortex activation during classic and emotional Stroop interference in child abuse-related complex post-traumatic stress disorder. Psychological medicine. 42:2337–2349. [PubMed: 22436595]
18. Aupperle RL, Allard CB, Simmons AN, Flagan T, Thorp SR, Norman SB, et al. (2013): Neural responses during emotional processing before and after cognitive trauma therapy for battered women. Psychiatry Res. 214:48–55. [PubMed: 23916537]
19. Simmons AN, Norman SB, Spadoni AD, Strigo IA (2013): Neurosubstrates of remission following prolonged exposure therapy in veterans with posttraumatic stress disorder. Psychotherapy and psychosomatics. 82:382–389. [PubMed: 24061484]
20. Brown VM, LaBar KS, Haswell CC, Gold AL, McCarthy G, Morey RA (2014): Altered resting-state functional connectivity of basolateral and centromedial amygdala complexes in posttraumatic stress disorder. Neuropsychopharmacology. 39:351–359. [PubMed: 23929546]
21. Sripada RK, King AP, Garfinkel SN, Wang X, Sripada CS, Welsh RC, et al. (2012): Altered resting-state amygdala functional connectivity in men with posttraumatic stress disorder. Journal of psychiatry & neuroscience : JPN. 37:241–249. [PubMed: 22313617]
22. Jin C, Qi R, Yin Y, Hu X, Duan L, Xu Q, et al. (2014): Abnormalities in whole-brain functional connectivity observed in treatment-naive post-traumatic stress disorder patients following an earthquake. Psychological medicine. 44:1927–1936. [PubMed: 24168716]
23. Nicholson AA, Sapru I, Densmore M, Frewen PA, Neufeld RW, Theberge J, et al. (2016): Unique insula subregion resting-state functional connectivity with amygdala complexes in posttraumatic stress disorder and its dissociative subtype. Psychiatry research Neuroimaging. 250:61–72. [PubMed: 27042977]

24. Ghaziri J, Tucholka A, Girard G, Boucher O, Houde J-C, Descoteaux M, et al. (2018): Subcortical structural connectivity of insular subregions. Scientific Reports. 8:8596. [PubMed: 29872212]
25. Baur V, Hänggi J, Langer N, Jäncke L (2013): Resting-State Functional and Structural Connectivity Within an Insula–Amygdala Route Specifically Index State and Trait Anxiety. Biological Psychiatry. 73:85–92. [PubMed: 22770651]
26. Kober H, Barrett LF, Joseph J, Bliss-Moreau E, Lindquist K, Wager TD (2008): Functional grouping and cortical-subcortical interactions in emotion: a meta-analysis of neuroimaging studies. Neuroimage. 42:998–1031. [PubMed: 18579414]
27. Berret E, Kintscher M, Palchaudhuri S, Tang W, Osypenko D, Kochubey O, et al. (2019): Insular cortex processes aversive somatosensory information and is crucial for threat learning. Science.eaaw0474. [PubMed: 31097492]
28. Sripada RK, King AP, Welsh RC, Garfinkel SN, Wang X, Sripada CS, et al. (2012): Neural dysregulation in posttraumatic stress disorder: evidence for disrupted equilibrium between salience and default mode brain networks. Psychosom Med. 74:904–911. [PubMed: 23115342]
29. Zhang Y, Liu F, Chen H, Li M, Duan X, Xie B, et al. (2015): Intranetwork and internetwork functional connectivity alterations in post-traumatic stress disorder. J Affect Disord. 187:114–121. [PubMed: 26331685]
30. Koch SB, van Zuiden M, Nawijn L, Frijling JL, Veltman DJ, Olff M (2016): ABERRANT RESTING-STATE BRAIN ACTIVITY IN POSTTRAUMATIC STRESS DISORDER: A META-ANALYSIS AND SYSTEMATIC REVIEW. Depression and anxiety. 33:592–605. [PubMed: 26918313]
31. Rabinak CA, Angstadt M, Welsh RC, Kenndy AE, Lyubkin M, Martis B, et al. (2011): Altered amygdala resting-state functional connectivity in post-traumatic stress disorder. Frontiers in psychiatry. 2:62. [PubMed: 22102841]
32. Bluhm RL, Williamson PC, Osuch EA, Frewen PA, Stevens TK, Boksman K, et al. (2009): Alterations in default network connectivity in posttraumatic stress disorder related to early-life trauma. Journal of psychiatry & neuroscience : JPN. 34:187–194. [PubMed: 19448848]
33. Zhu X, Suarez-Jimenez B, Lazarov A, Helpman L, Papini S, Lowell A, et al. (2018): Exposure-based therapy changes amygdala and hippocampus resting-state functional connectivity in patients with posttraumatic stress disorder. Depression and anxiety. 35:974–984. [PubMed: 30260530]
34. King AP, Block SR, Sripada RK, Rauch S, Giardino N, Favorite T, et al. (2016): ALTERED DEFAULT MODE NETWORK (DMN) RESTING STATE FUNCTIONAL CONNECTIVITY FOLLOWING A MINDFULNESS-BASED EXPOSURE THERAPY FOR POSTTRAUMATIC STRESS DISORDER (PTSD) IN COMBAT VETERANS OF AFGHANISTAN AND IRAQ. Depression and anxiety. 33:289–299. [PubMed: 27038410]
35. Misaki M, Phillips R, Zotev V, Wong CK, Wurfel BE, Krueger F, et al. (2018): Real-time fMRI amygdala neurofeedback positive emotional training normalized resting-state functional connectivity in combat veterans with and without PTSD: a connectome-wide investigation. Neuroimage Clin. 20:543–555. [PubMed: 30175041]
36. Shou H, Yang Z, Satterthwaite TD, Cook PA, Bruce SE, Shinohara RT, et al. (2017): Cognitive behavioral therapy increases amygdala connectivity with the cognitive control network in both MDD and PTSD. Neuroimage Clin. 14:464–470. [PubMed: 28275546]
37. Yang Z, Gu S, Honnorat N, Linn KA, Shinohara RT, Aselcioglu I, et al. (2018): Network changes associated with transdiagnostic depressive symptom improvement following cognitive behavioral therapy in MDD and PTSD. Mol Psychiatry. 23:2314–2323. [PubMed: 30104727]
38. Etkin A, Wager TD (2007): Functional neuroimaging of anxiety: a meta-analysis of emotional processing in PTSD, social anxiety disorder, and specific phobia. Am J Psychiatry. 164:1476–1488. [PubMed: 17898336]
39. Patel R, Spreng RN, Shin LM, Girard TA (2012): Neurocircuitry models of posttraumatic stress disorder and beyond: a meta-analysis of functional neuroimaging studies. Neurosci Biobehav Rev. 36:2130–2142. [PubMed: 22766141]
40. Fenster RJ, Lebois LAM, Ressler KJ, Suh J (2018): Brain circuit dysfunction in post-traumatic stress disorder: from mouse to man. Nature Reviews Neuroscience.

41. Disner SG, Marquardt CA, Mueller BA, Burton PC, Sponheim SR (2018): Spontaneous neural activity differences in posttraumatic stress disorder: A quantitative resting-state meta-analysis and fMRI validation. Hum Brain Mapp. 39:837–850. [PubMed: 29143411]
42. Hayes JP, Hayes SM, Mikedis AM (2012): Quantitative meta-analysis of neural activity in posttraumatic stress disorder. Biology of mood & anxiety disorders. 2:9. [PubMed: 22738125]
43. Etkin A, Maron-Katz A, Wu W, Fonzo GA, Huemer J, Vertes PE, et al. (2019): Using fMRI connectivity to define a treatment-resistant form of post-traumatic stress disorder. Sci Trans! Med. 11:eaal3236.
44. Friston KJ, Harrison L, Penny W (2003): Dynamic causal modelling. NeuroImage. 19:1273–1302. [PubMed: 12948688]
45. Friston KJ, Kahan J, Biswal B, Razi A (2014): A DCM for resting state fMRI. Neuroimage. 94:396–407. [PubMed: 24345387]
46. Blake DD, Weathers FW, Nagy LM, Kaloupek DG, Gusman FD, Charney DS, et al. (1995): The development of a Clinician-Administered PTSD Scale. Journal of traumatic stress. 8:75–90. [PubMed: 7712061]
47. First MB, Spitzer RL, Gibbon M, Williams JBW (2002): Structured Clinical Interview for DSM-IV-TR Axis I Disorders, Research Version, Patient Edition (SCID-I/P). New York: Biometrics Research, New York State Psychiatric Institute.
48. Foa EB, Hembree EA, Rothbaum BO, Rauch SA (2019): Prolonged Exposure Therapy for PTSD: Emotional Processing of Traumatic Experiences. Second ed. Oxford: Oxford University Press.
49. Whitfield-Gabrieli S, Nieto-Castanon A (2012): Conn: a functional connectivity toolbox for correlated and anticorrelated brain networks. Brain Connect. 2:125–141. [PubMed: 22642651]
50. Amunts K, Kedo O, Kindler M, Pieperhoff P, Mohlberg H, Shah NJ, et al. (2005): Cytoarchitectonic mapping of the human amygdala, hippocampal region and entorhinal cortex: intersubject variability and probability maps. Anatomy and embryology. 210:343–352. [PubMed: 16208455]
51. Chang LJ, Yarkoni T, Khaw MW, Sanfey AG (2013): Decoding the role of the insula in human cognition: functional parcellation and large-scale reverse inference. Cerebral cortex (New York, NY: 1991). 23:739–749.
52. Chen G, Saad ZS, Britton JC, Pine DS, Cox RW (2013): Linear mixed-effects modeling approach to FMRI group analysis. Neuroimage. 73:176–190. [PubMed: 23376789]
53. Almgren H, Van de Steen F, Razi A, Friston K, Marinazzo D (2019): The effect of global signal regression on DCM estimates of noise and effective connectivity from resting state fMRI. NeuroImage.116435. [PubMed: 31816423]
54. Zeidman P, Jafarian A, Seghier ML, Litvak V, Cagnan H, Price CJ, et al. (2019): A guide to group effective connectivity analysis, part 2: Second level analysis with PEB. NeuroImage.
55. Friston K, Penny W (2011): Post hoc Bayesian model selection. NeuroImage. 56:2089–2099. [PubMed: 21459150]
56. Penny WD, Stephan KE, Daunizeau J, Rosa MJ, Friston KJ, Schofield TM, et al. (2010): Comparing families of dynamic causal models. PLoS computational biology. 6:e1000709. [PubMed: 20300649]
57. Friston KJ, Litvak V, Oswal A, Razi A, Stephan KE, van Wijk BCM, et al. (2016): Bayesian model reduction and empirical Bayes for group (DCM) studies. NeuroImage. 128:413–431. [PubMed: 26569570]
58. Schaefer A, Kong R, Gordon EM, Laumann TO, Zuo XN, Holmes AJ, et al. (2017): Local-Global Parcellation of the Human Cerebral Cortex from Intrinsic Functional Connectivity MRI. Cerebral cortex (New York, NY: 1991).1–20.
59. Morey RA, Petty CM, Cooper DA, Labar KS, McCarthy G (2008): Neural systems for executive and emotional processing are modulated by symptoms of posttraumatic stress disorder in Iraq War veterans. Psychiatry Res. 162:59–72. [PubMed: 18093809]
60. Morey RA, Dolcos F, Petty CM, Cooper DA, Hayes JP, LaBar KS, et al. (2009): The role of trauma-related distractors on neural systems for working memory and emotion processing in posttraumatic stress disorder. J Psychiatr Res. 43:809–817. [PubMed: 19091328]

61. Muhle-Karbe PS, Derrfuss J, Lynn MT, Neubert FX, Fox PT, Brass M, et al. (2015): Co-Activation-Based Parcellation of the Lateral Prefrontal Cortex Delineates the Inferior Frontal Junction Area. Cerebral Cortex. 26:2225–2241. [PubMed: 25899707]

62. Yeo BT, Krienen FM, Sepulcre J, Sabuncu MR, Lashkari D, Hollinshead M, et al. (2011): The organization of the human cerebral cortex estimated by intrinsic functional connectivity. J Neurophysiol. 106:1125–1165. [PubMed: 21653723]

63. Frassle S, Lomakina EI, Razi A, Friston KJ, Buhmann JM, Stephan KE (2017): Regression DCM for fMRI. Neuroimage. 155:406–421. [PubMed: 28259780]

64. Razi A, Seghier ML, Zhou Y, McColgan P, Zeidman P, Park HJ, et al. (2017): Large-scale DCMs for resting-state fMRI. Network neuroscience (Cambridge, Mass). 1:222–241.

65. Stephan KE, Penny WD, Moran RJ, den Ouden HE, Daunizeau J, Friston KJ (2010): Ten simple rules for dynamic causal modeling. Neuroimage. 49:3099–3109. [PubMed: 19914382]

66. Stefanacci L, Amaral DG (2002): Some observations on cortical inputs to the macaque monkey amygdala: an anterograde tracing study. J Comp Neurol. 451:301–323. [PubMed: 12210126]

67. Ray RD, Zald DH (2012): Anatomical insights into the interaction of emotion and cognition in the prefrontal cortex. Neurosci Biobehav Rev. 36:479–501. [PubMed: 21889953]

68. Gehrlach DA, Dolensek N, Klein AS, Roy Chowdhury R, Matthys A, Junghänel M, et al. (2019): Aversive state processing in the posterior insular cortex. Nature Neuroscience. 22:1424–1437. [PubMed: 31455886]

69. Saygin ZM, Osher DE, Koldewyn K, Martin RE, Finn A, Saxe R, et al. (2015): Structural Connectivity of the Developing Human Amygdala. PLOS ONE. 10:e0125170. [PubMed: 25875758]

70. Mégevand P, Groppe DM, Bickel S, Mercier MR, Goldfinger MS, Keller CJ, et al. (2017): The Hippocampus and Amygdala Are Integrators of Neocortical Influence: A CorticoCortical Evoked Potential Study. Brain connectivity. 7:648–660. [PubMed: 28978234]

71. Aggleton JP, Burton MJ, Passingham RE (1980): Cortical and subcortical afferents to the amygdala of the rhesus monkey (Macaca mulatta). Brain Res. 190:347–368. [PubMed: 6768425]

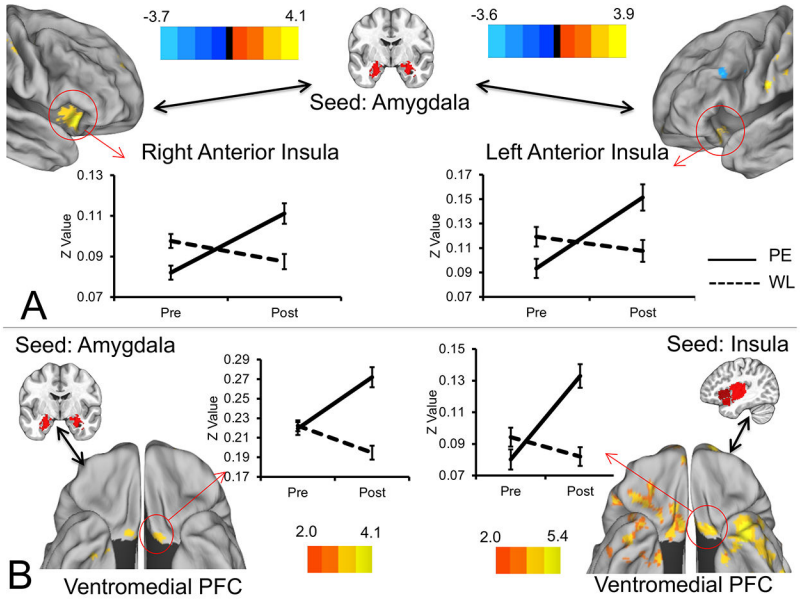

Figure 1.

Treatment-related increases in intrinsic connectivity of the insula and amygdala with each other and with the posterior ventromedial prefrontal cortex. Figure depicts regions of the insula displaying treatment-related increases in intrinsic connectivity with the amygdala (A), and regions of the posterior ventromedial prefrontal cortex displaying increased connectivity with both the amygdala and insula (B). FDR-corrected Z values for the treatment arm x time effect are rendered on an average brain surface with signs indicating the directionality of change in the prolonged exposure arm. Positive Z values indicate greater connectivity in the prolonged exposure arm at post-treatment vs. pre-treatment, whereas negative signs indicate greater connectivity at pre-treatment vs. post-treatment. Seed regions are displayed on the MNI average brain. Error bars indicate ± 1 S.E. PE = prolonged exposure; PFC = prefrontal cortex; Post = post-treatment; Pre = pre-treatment; WL = waiting list.

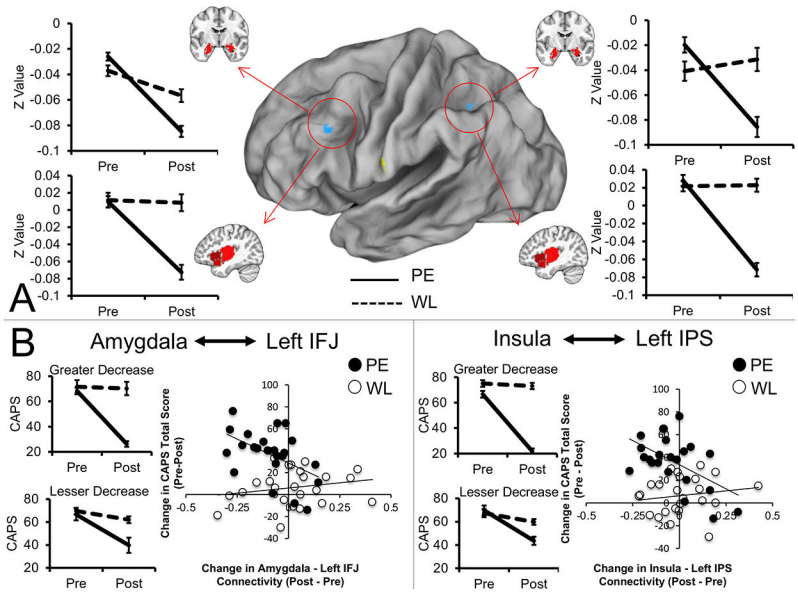

Figure 2.

Treatment-related decreases in intrinsic connectivity of both the amygdala and insula with fronto-parietal regions and associations with treatment response. Figure depicts regions of the left IFJ and left IPS that displayed treatment-related decreases in connectivity with both the amygdala and insula, identified via conjunction analysis (A). Solid lines are the prolonged exposure arm and dotted lines represent the waiting list arm. Of these effects, greater decreases in amygdala-left IFJ connectivity and greater decreases in insula-left IPS connectivity were associated with larger reductions in CAPS Total scores from pre- to post-treatment (B). Graphs in B display changes in CAPS total scores from pre- to post-treatment with separate plots for individuals from each treatment arm above and below the grand mean for the connectivity decreases. Note this median split is done for visual purposes only, and the analysis treated connectivity change as a continuous variable. Scatter plots depicting the relationships between change in connectivity (post-treatment vs. pre-treatment) and change in Clinician-Administered PTSD Scale total scores (pre-treatment vs. post-treatment) are also displayed for additional visualization of relationships. Note that these reflect data from completers only and are thus not directly comparable to results from the mixed model analyses. Areas from conjunction analysis are rendered on an average brain surface with signs indicating the directionality of change in the prolonged exposure arm (blue denoting less connectivity at post-treatment, yellow denoting greater connectivity at post-treatment). Seed regions are displayed on the MNI average brain. Error bars indicate ± 1 S.E. CAPS = Clinician-Administered PTSD Scale; IFJ = inferior frontal junction; IPS = intraparietal sulcus; PE = prolonged exposure; Pre = pre-treatment; Post = post-treatment; WL = waiting list.

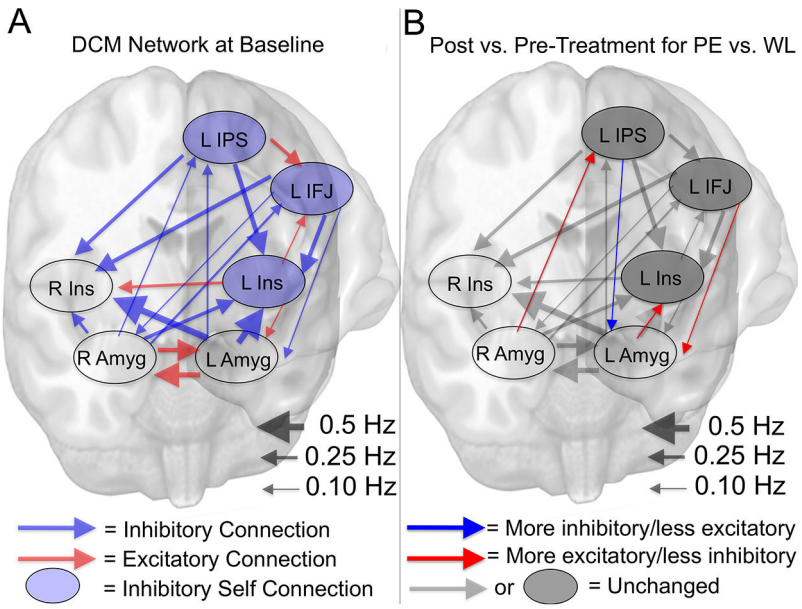

Figure 3.

Baseline effective connectivity parameters of DCM network and differential modulation of time-related changes by treatment arm. The picture in A depicts the baseline effective connectivity parameters of the DCM network encompassing the left and right amygdala and insula as well as the left IFJ and left IPS regions found to display uniform treatment-related decreases in intrinsic connectivity that were associated with PTSD symptom changes. Only connections with strong evidence (posterior probabilities > 0.95) are depicted. Blue lines indicate inhibitory influences while red lines indicate excitatory influences. Shaded blue circles indicate inhibitory self -connections with strong evidence. Lines are scaled by the strength of the parameter from 0 to 0.5 Hz. Picture in B depicts the same network structure overlaid with parameters that displayed strong evidence (posterior probabilities > 0.95) for differential time-related modulation as a function of treatment arm, i.e. a treatment arm x time effect. Connections overlaid with an additional red arrow indicate a greater time-related shift from pre- to post-treatment towards more excitation/less inhibition for prolonged exposure vs. waiting list, while connections overlaid with an additional blue arrow indicate a greater time-related shift from pre- to post-treatment towards more inhibition/less excitation for prolonged exposure vs. waiting list. Connections in black/grey indicate no strong evidence for a differential time-related modulation of connection strength as a function of treatment arm. Amyg = amygdala; DCM = dynamic causal modeling; Hz = hertz; IFJ = inferior frontal junction; IPS = intraparietal sulcus; Ins = Insula; L = left; PE = prolonged exposure; R = right; WL = waiting list.

Table 1.

Participant demographics and treatment outcome.

Measure	Immediate Treatment (N=36)	Patient Waitlist (N=30)	F/χ^2 (p value)	Cohen's d (95% CI)
	Mean or N and % of Group (SD)	Mean or N and % of Group (SD)		
Age (yrs)	34.42 (10.23)	39.03 (10.35)	--	--
Education (yrs)	14.72 (2.17)	15.17 (2.78)	--	--
Sex	Male (N=13; 36%)	Male (N=10; 33%)	--	--
	Female (N=23; 64%)	Female (N=20; 66%)		
WASI Full Scale IQ	109.03 (9.09)	112.81 (11.57)	--	--
SSRI/SNRI Meds	Sertraline (N=1; 3%)	Duloxetine (N=1; 3%)	--	--
	Citalopram (N=2; 5%)	Sertraline (N=1; 3%)		
MDD Diagnosis at Intake	Yes (N=18; 50%)	Yes (N=17; 57%)	--	--
	No (N=18; 50%)	No (N=13; 43%)		
Dropout	Completed (N=25; 69%)	Completed (N=26; 87%)	--	--
	Did not complete (N=11; 31%)	Did not complete (N=4; 13%)		
CAPS Index Trauma	Natural disaster (N=3; 8%)	Natural disaster (N=1; 3%)	--	--
	Physical Assault (N=9; 25%)	Physical assault (N=7; 23%)		
	Assault w/ weapon (N=3; 8%)	Assault w/ weapon (N=2; 7%)		
	Sexual assault (N=12; 33%)	Sexual assault (N=9; 30%)		
	Combat exposure (N=4; 11%)	Combat exposure (N=4; 13%)		
	Injury/illness/suffering (N=5; 14%)	Injury/illness/suffering (N=7; 23%)		
Pre-Treatment Symptom/Quality of Life Measures				
CAPS: Developmental Stage at Time of Index Trauma	Adult (N=20; 56%)	Adult (N=14; 47%)	--	--
	Teen (N=8; 22%)	Teen (N=11; 37%)		
	Child (N=8; 22%)	Child (N=5; 17%)		
CAPS: How Exposed to Index Trauma	Experienced (N=27; 75%)	Experienced (N=17; 57%)	--	--
	Witnessed (N=9; 25%)	Witnessed (N=13; 43%)		
CAPS: Index Trauma Repeated?	No (N=25; 69%)	No (N=20; 66%)	--	--
	Yes (N=11; 31%)	Yes (N=10; 33%)		
CAPS: Multiple Criterion A Events?	No (N=24; 66%)	No (N=20; 66%)	--	--
	Yes (N=12; 33%)	Yes (N=10; 33%)		
CAPS Total	66.33 (15.17)	71.37 (14.99)	--	--
CAPS ReExp	17.53 (6.40)	18.73 (6.02)	--	--
CAPS Avd	26.94 (7.86)	28.77 (8.89)	--	--
CAPS Hyper	21.86 (6.28)	23.87 (4.91)	--	--
BDI-II Total	23.69 (8.68)	23.17 (8.60)	--	--
PCL-C Total	56.16 (10.61)	57.36 (12.04)	--	--

Measure	Immediate Treatment (N=36)	Patient Waitlist (N=30)	F/χ^2 (p value)	Cohen's d (95% CI)
	Mean or N and % of Group (SD)	Mean or N and % of Group (SD)		
PCL-C ReExp	16.47 (3.83)	16.29 (3.98)	--	--
PCL-C Avd	22.78 (5.05)	23.04 (6.02)	--	--
PCL-C Hyper	16.91 (4.22)	18.04 (4.19)	--	--
WHO-QoL Physical	12.46 (2.99)	12.43 (3.11)	--	--
WHO-QoL Psych	10.04 (2.29)	10.83 (2.34)	--	--
WHO-QoL SocRx	9.71 (4.06)	9.29 (3.51)	--	--
WHO-QoL Envir	12.30 (3.48)	12.79 (3.37)	--	--
Post-Treatment Symptom/Quality of Life Measures				
CAPS Total	29.60 (21.26)	64.23 (21.77)	32.99 (< 0.001) ***	1.61 (1.14, 2.08)
CAPS ReExp	6.20 (6.49)	16.92 (7.97)	27.62 (< 0.001) ***	1.48 (1.03, 1.92)
CAPS Avd	10.60 (9.50)	24.50 (11.30)	22.51 (< 0.001) ***	1.33 (0.92, 1.74)
CAPS Hyper	12.80 (8.75)	22.81 (7.00)	20.43 (< 0.001) ***	1.26 (0.86, 1.66)
BDI-II Total	9.69 (7.77)	17.87 (9.27)	11.23 (0.002) **	0.96 (0.60, 1.31)
MASQ Gen Dis	20.43 (9.39)	28.38 (8.89)	8.68 (0.004) **	0.87 (0.51,1.23)
MASQ Anh Dep	33.21 (8.63)	35.95 (7.94)	2.93 (0.09)	0.33 (0.08, 0.58)
MASQ Anx Aro	16.52 (7.2)	22.09 (8.01)	6.29 (0.014) *	0.73 (0.40, 1.06)
PCL-C Total	26.13 (7.80)	49.00 (13.35)	45.55 (< 0.001) ***	2.09 (1.45, 2.73)
PCL-C ReExp	7.41 (2.63)	14.38 (5.14)	31.76 (< 0.001) ***	1.71 (1.16, 2.26)
PCL-C Avd	10.36 (3.36)	19.24 (6.32)	33.46 (< 0.001) ***	1.75 (1.19, 2.32)
PCL-C Hyper	8.41 (3.11)	15.38 (4.15)	39.05 (< 0.001) ***	1.90 (1.31, 2.49)
WHO-QoL Physical	14.63 (3.29)	12.65 (3.19)	4.09 (0.049) *	0.61 (0.30, 0.92)
WHO-QoL Psych	13.19 (2.59)	11.94 (2.52)	2.63 (0.11)	0.49 (0.21, 0.77)
WHO-QoL SocRx	11.83 (3.20)	10.73 (3.20)	1.29 (0.26)	0.34 (0.09, 0.59)
WHO-QoL Envir	14.59 (2.42)	13.57 (2.99)	1.55 (0.22)	0.38 (0.12, 0.63)

Avd = avoidance/numbing subscale; BDI-II = Beck Depression Inventory-II; CAPS = Clinician-Administered PTSD Scale for DSM-IV; Hyper = hyperarousal subscale; MASQ Anh Dep = Anhedonic Depression subscale of Mood and Anxiety Symptom Questionnaire; MASQ Anx Aro = Anxious Arousal Subscale of Mood and Anxiety Symptom Questionnaire; MASQ Gen Dis = General Distress subscale of Mood and Anxiety Symptom Questionnaire; MDD = major depressive disorder; PCL = PTSD Checkist for DSM-IV Civilian Version; ReExp = reexperiencing subscale; SSRI = selective serotonin reuptake inhibitor; SNRI = serotonin/norepinephrine reuptake inhibitor; WASI = Wechsler Abbreviated Scale of Intelligence; WHO-QoL = WHO Quality of Life BREF Scale; WHO-Qol Physical = physical health subscale; WHO-QoL Psych = psychological health subscale; WHO-QoL SocRx = social relationships subscale; WHO-QoL Environ = environment subscale

* $p < 0.05$

** $p < 0.01$

*** $p < 0.001$.